Adsorption (2008) 14: 771–779
DOI 10.1007/s10450-007-9084-7

Adsorption of chlorobenzene vapor on V_2O_5/Al_2O_3 catalyst under dynamic conditions

Leonid Asnin · Anatoly Fedorov · Dina Yakusheva

Received: 25 January 2007 / Revised: 23 November 2007 / Accepted: 18 December 2007 / Published online: 23 April 2008

Abstract Adsorption dynamics of chlorobenzene vapors on a 5% V_2O_5/Al_2O_3 catalyst has been investigated using the frontal chromatography technique. The uptakes of chlorobenzene have been measured as a function of vapor concentration and adsorption equilibrium has been found to follow formally the Langmuir isotherm. The breakthrough time proved to be a linear function of the column length as expected. Breakthrough profiles have been reported for different experimental conditions and quantitatively fitted by a reduced lumped diffusion model. This model provides an analytical solution that facilitates engineering calculations. Model parameters show complex behavior as functions of stream characteristics and depend on column length. When empirical expressions relating model mass transfer coefficients with influencing variables are found the model demonstrates good accuracy in predicting column performance.

Keywords Adsorbents · Diffusion and kinetics

Abbreviations

a_p	specific external surface area of particles, $cm^2\ cm^{-3}$
b	adsorption constant in the Langmuir isotherm, $l\,g^{-1}$
Bi	Biot number
c	concentration in gas phase, $g\,l^{-1}$
D	internal diffusion coefficient, $cm^2\ min^{-1}$
D_{ax}	axial diffusion coefficient, $cm^2\ min^{-1}$
D_K	Knudsen diffusion coefficient, $cm^2\ min^{-1}$
D_{Km}	combined diffusion coefficient, $cm^2\ min^{-1}$
$\overline{D}_{Km}$	combined diffusion coefficient averaged over pore size, $cm^2\ min^{-1}$
D_m	molecular diffusion coefficient, $cm^2\ min^{-1}$
d_p	average particle diameter, cm
h	parameter of the dimensionless Langmuir isotherm
K	slope coefficient in (5), $min\,cm^{-1}$
K_1, K_2	coefficients defined by (6), min
L	column length, cm
Pe	Peclet number
q	concentration in solid phase, g (l bed volume)$^{-1}$
$q^\star$	saturation capacity of the adsorbent in the Langmuir isotherm, g (l bed volume)$^{-1}$
r	pore radius, cm
r_1, r_2	the lower and upper limit of a pore size distribution respectively, cm
R^2	coefficient of determination
St	Stanton number
T	temperature, °C
t	time, min
t_0	intercept in (5), min
u	c/c^0, dimensionless concentration in moving gas phase
v	superficial flow velocity, $cm\,min^{-1}$
x	axial coordinate, cm
z_1, z_2	variables defined by (7) and (8) respectively

Greek symbols

β_e	external mass transfer coefficient, min^{-1} (l gas phase) (l bed volume)$^{-1}$
β_i	internal mass transfer coefficient, min^{-1}

L. Asnin (✉) · A. Fedorov · D. Yakusheva
Institute of Technical Chemistry, Ural Branch of the Russian Academy of Sciences, Perm 614990, Russia
e-mail: asninld@mail.ru

β_k	$k = 0, 1, 2, 3$, adjustable coefficients defined in Table 7
$\delta_j, \delta_{jk}, \delta_{jkl}$	$j, k, l = 0, 1, 2, 3$, adjustable coefficients defined in Table 7
Γ	adsorption constant, (l gas phase) (l bed volume)$^{-1}$
ϵ_e	external porosity
ϵ_p	particle porosity

Superscripts

0	feed
s	surface

1 Introduction

Combined adsorption and catalytic oxidation technology is considered to be the method of choice for purification of industrial waste gases from low-concentrated admixtures of volatile organic compounds (VOC) (Zagoruiko et al. 1986; Chintavar and Green 1997; Xia et al. 2001). For instance, this method has been recommended (Fedorov et al. 1998) for the neutralization of gaseous wastes containing chlorobenzene (CB), which is the pollutant of interest in the present work.

In an adsorption-catalytic process a contaminant is first accumulated on a catalyst under ambient conditions, followed by oxidative destruction to harmless products by the increase of temperature and, optionally, by additional feed of an oxidant into the reactor. To avoid any breakthrough the adsorption step has to be terminated till a target component reaches the end of the catalyst bed, even a certain additional "safe" length of the bed should be provided. Thus, a proper development of the process requires the knowledge of the shape and rate of propagation of the adsorption front. However, studies on column dynamics of VOCs are very limited (Shim et al. 2005). Particularly, there is a lack of proper information concerning chlorobenzenes. Thereupon our aim here is to investigate adsorption dynamics for CB vapors on a V_2O_5/Al_2O_3 catalyst. Vanadia materials are known to be active in deep oxidation of chlorinated organics (Everaert and Baeyens 2004; Krishnamoorthy et al. 1998). In spite of alumina supported catalysts showing lower activity as compared with those based on TiO_2 (Krishnamoorthy and Amiridis 1999) or ZrO_2-Al_2O_3 supports (Jones and Ross 1997), they are attractive due to higher specific surface and low cost.

Contrary to dynamic studies, the mechanism of mono(di)-chlorobenzene adsorption on V_2O_5/Al_2O_3 is well studied using the IR, FTIR and temperature-programmed desorption methods (Davidenko et al. 1990, 1991; Krishnamoorthy and Amiridis 1999). In general, CB is adsorbed in a molecular form at ambient temperature so that the benzene ring lies in parallel to the surface, and the adsorption is dissociative at temperature above 300 °C. The adsorption equilibrium in helium atmosphere has been studied on a catalyst containing 5% V_2O_5 within the temperature range 190–240 °C at CB partial pressure under 18 Pa (Asnin et al. 2001). Even at such low partial pressure adsorption isotherms are nonlinear, obeying to Freundlich equation.

2 Theoretical

The reduced lumped diffusion model (Akulov et al. 1986) applied to explain breakthrough curves is defined by the following set of equations:

$$\frac{\partial q}{\partial t} + \epsilon_e \frac{\partial c}{\partial t} + v \frac{\partial c}{\partial x} = 0 \tag{1}$$

$$\frac{\partial q}{\partial t} = \beta_e (c - c^s) = \beta_i (q^s - q) \tag{2}$$

$$q = f(c) \tag{3}$$

where (3) represents an adsorption isotherm. The initial and boundary conditions are given by

$$q(x, 0) = 0, \qquad c(0, t) = c^0 \tag{4}$$

Note that equilibrium conditions are assumed between the stagnant fluid film and the adsorbed phase at the external surface of a catalyst particle, so that $q^s = f(c^s)$.

The model differs from the classic lumped diffusion (POR) model (Morbidelli et al. 1984; Kaczmarski et al. 2001) by neglecting the axial dispersion term in the mass-balance equation. This simplification allows developing an analytical solution but it might affect the numerical values of the model parameters to a degree. This phenomenon is well known in chromatography and has been comprehensively discussed (Golshan-Shirazi and Guiochon 1992; Guiochon 2002). The error is obviously low when the contribution of the axial dispersion in saturation front broadening is small compared to the mass transfer kinetics contribution. From an engineering point of view, apparent nature of model parameters is not an obstacle while a model predicts breakthrough curves. Although it may be difficult to use the values of the rate coefficients for understanding the mass transfer mechanism and the kinetics of its different steps. Useful information is then derived from observations of trends in the coefficients due to a change of experimental conditions.

The model also assumes that (1) the chromatographic process is isothermal, (2) the concentration gradient in the radial direction of the bed is negligible, (3) only transport pores (macro and mesopores) contribute into the internal mass-transfer resistance and surface diffusion is to be neglected, and (4) the mobile phase velocity is constant. The

latter assumption is well admissible as the pressure drop across the column was less than 10% of the atmospheric pressure.

Lukin and Novoselskii (1989) developed an analytical solution of the model for a case of spherical particles of uniform size and the Langmuir adsorption isotherm that reads

$$t(u) = KL - t_0(u) \tag{5}$$

Coefficient $K = \Gamma/v$ is reciprocal of the rate of propagation of the adsorption front, $\Gamma = q^0/c^0$ being the adsorption constant. Intercept $t_0(u)$ is a linear combination of the variables $z_1(u)$ and $z_2(u)$

$$t_0(u) = K_1 z_1(u) + K_2 z_2(u) \tag{6}$$

$$z_1(u) = \ln\frac{1}{u} - 1 + h\ln\frac{1-u}{u} \tag{7}$$

$$\begin{aligned} z_2(u) = {} & \frac{3}{2}(1-u)^{2/3} + u - \frac{7}{5} \\ & + h\cdot\left[\frac{3}{2}\ln(1+(1-u)^{1/3}+(1-u)^{2/3})\right. \\ & \left. - \sqrt{3}\arctan\frac{2(1-u)^{1/3}+1}{\sqrt{3}} - \frac{1}{2} + \frac{\pi}{2\sqrt{3}}\right] \end{aligned} \tag{8}$$

where $u = c/c^0$, h is the parameter of the Langmuir isotherm written in a dimensionless form (q^0 is the solid phase concentration in equilibrium with the concentration c^0)

$$(q/q^0) = \frac{(1+h)u}{h+u} \tag{9}$$

The constants $K_1 = \Gamma/\beta_e$ and $K_2 = \Gamma d_p^2/(12D)$ are proportional to the external and internal mass-transfer resistance respectively.

3 Experimental

The protocol of catalyst preparation has been described previously (Asnin et al. 2001). The only difference is the use of technical alumina (Industrial Catalysts, Ryazan, Russia) instead of home-made γ-Al_2O_3 as a support in this investigation. The qualities of the catalyst were examined by the nitrogen adsorption-desorption technique (Micromeritics ASAP 2400) and listed in Table 1.

Breakthrough curves were measured using a "Tsvet-530" gas chromatograph (Tsvet, USSR) equipped with a flame-ionization detector and a heated four-way valve that switched a flow entering an adsorption column between a pure carrier gas and a gaseous feed mixture thus allowing a frontal analysis (FA) mode. The experiments were carried out at 50 and 100 °C. Detector response was recorded using a computer data acquisition system governed by the PowerGraph 2.0 software (Interoptika-C Ltd., Russia). The adsorption column was of brass, 5, 10 or 15 cm long, 0.9 cm i.d. packed with the catalyst in the form of 0.063–0.080 cm particles. Prior to each run, the column was conditioned in the pure carrier gas for 8 h at 150 °C. Nitrogen, used as a carrier gas, was purified by passing through successively connected traps with alumina and CaA zeolite. CB (analytical pure grade) was additionally dried over NaA zeolite. The gas-vapor mixture was prepared by the passage of nitrogen through a saturator containing CB maintained at 0 °C. This saturated stream was mixed with nitrogen to achieve the desired concentration. Weight control of the saturator before and after experiment gave mass flux of the adsorbate. Breakthrough was defined as the time when response corresponding to 0.1% of c^0 was first detected. Equilibrium adsorbed amount was determined as usual in FA by means of integrating of a breakthrough curve. A correction for hold-up time as evaluated with respect to methane was taken into account in all the calculations.

Table 1 Details of V_2O_5/Al_2O_3 catalyst

Surface area/$m^2\ g^{-1}$	213
Macropores/$cm^3\ g^{-1}$	0.01
Mesopores/$cm^3\ g^{-1}$	0.61
Total pore volume/$cm^3\ g^{-1}$	0.62
Particle porosity	0.66

4 Results and discussion

Pore size distribution for the catalyst is reported in Fig. 1, showing the two distinct peaks related to mesopores. No micropores were found within the limits of sensitivity of the equipment. Adsorption characteristics of the sample measured under different experimental conditions are collected in Table 2. Equilibrium data demonstrate a good reproducibility, the breakthrough adsorption capacity is more fluctuating but independence of the value from the column length is evident. The adsorption characteristics are independent of the flow rate but are influenced by the chlorobenzene concentration in the feed flow. The ratio of the equilibrium to breakthrough adsorption capacities is ~ 1.15 and is invariable under experimental conditions investigated. Thus, about 13% of adsorption capacity is not effectively used under dynamic conditions. The capacity of the catalysts decreases 3 times when temperature increases from 50 to 100 °C, other conditions being equal. The equilibrium data plotted in the coordinates of the linear form of the Langmuir

Table 2 A summary of the variation in adsorption capacity with column length and flow conditions

Flow rate(*)/	Concentration/	Breakthrough adsorption capacity(**)/g g^{-1}			Equilibrium adsorption capacity(***)/g g^{-1}		
ml min^{-1}	g l^{-1}	$L = 5$ cm	$L = 10$ cm	$L = 15$ cm	$L = 5$ cm	$L = 10$ cm	$L = 15$ cm
$T = 50$ °C							
62.5	0.0143	0.0483	0.0508		0.0539	0.0532	
92.7	0.0143		0.0503			0.0532	
94.5	0.0094	0.0410	0.0441		0.0470	0.0463	
$T = 100$ °C							
37.5	0.0123	0.0164	0.0165	0.0167	0.0180	0.0178	0.0183
75.0	0.0065	0.0117	0.0127	0.0118	0.0137	0.0135	0.0134
75.0	0.0126	0.0160	0.0164	0.0159	0.0183	0.0180	0.0183
110	0.0040	0.082	0.096		0.0098	0.0104	
110	0.0084	0.0124	0.0142	0.0130	0.0148	0.0157	0.0153
110	0.0124		0.0165	0.0154		0.0180	0.0182

(*) Volumetric
(**) Specific amount of vapors adsorbed at breakthrough
(***) Specific amount of vapors adsorbed at saturation

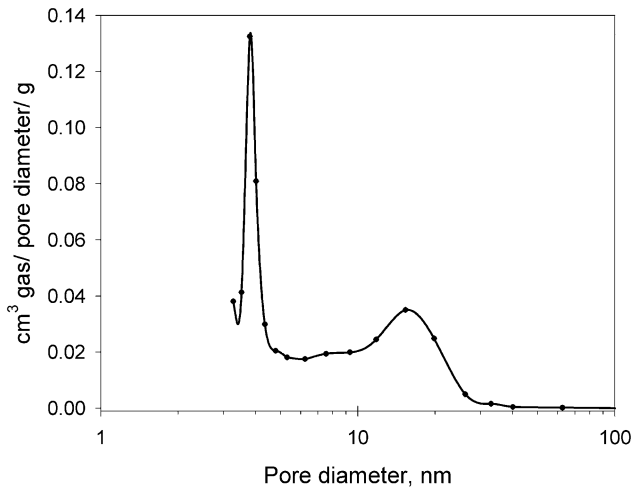

Fig. 1 Differential pore size distribution

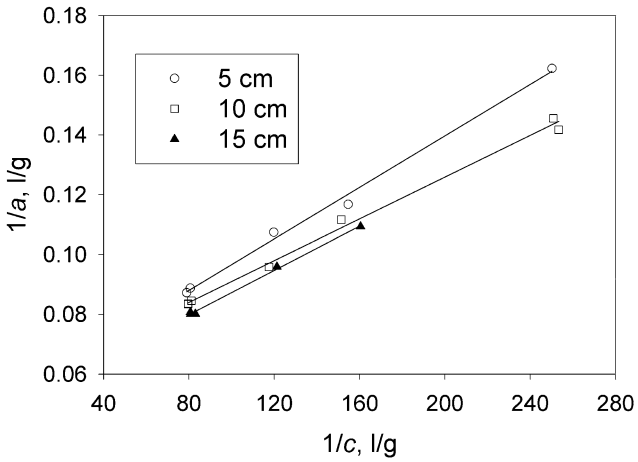

Fig. 2 Adsorption isotherms of chlorobenzene in reciprocal scale measured with columns of different lengths at 100 °C. *Lines* show approximation by the Langmuir equation

adsorption isotherm,

$$\frac{1}{q} = \frac{1}{q^\star bc} + \frac{1}{q^\star}, \tag{10}$$

are straight lines although the results for each column length are somewhat different (Fig. 2) that can be accounted for experimental errors. The values derived for the isotherm parameters are summarized in Table 3.

Table 3 Parameters of the Langmuir adsorption isotherm at $T = 100$ °C

L/cm	5	10	15	All(*)
$q^\star$/g l^{-1}	18.66	17.83	19.87	18.97
b/l g^{-1}	124.5	160.6	136.2	136.6

(*) Determined by data of all column lengths

The fact that adsorption data are well approximated by the Langmuir isotherm does not mandatory imply assumptions of the Langmuir model (adsorption on a homogeneous surface) to be valid. Indeed, earlier (Asnin et al. 2001) it was found that chlorobenzene adsorption on a vanadia/alumina catalyst at low surface coverage obeyed to the Freundlich isotherm. Two explanations are possible. The first one is that within a narrow range of the data obtained, surface coverage values being from 0.1 to 0.2, deviations from the Langmuir model are not visible. On the other hand, it has been men-

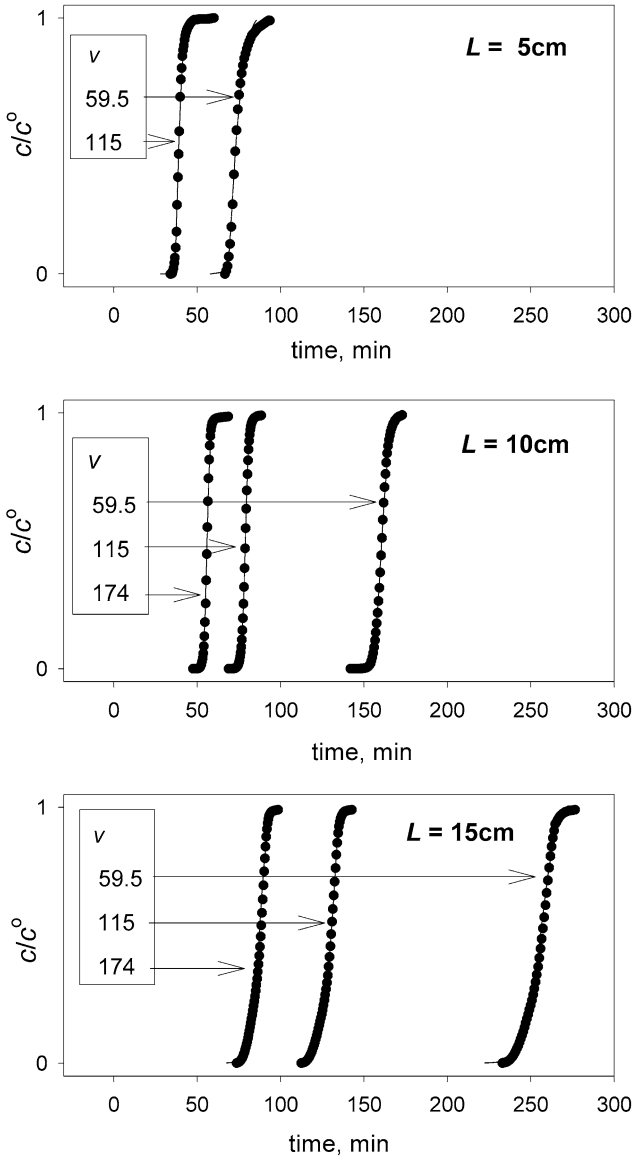

Fig. 3 The effect of flow rate and column length on breakthrough curves of chlorobenzene. *Points* represent the experimental data, *lines* are best-fit profiles determined using (5–8)

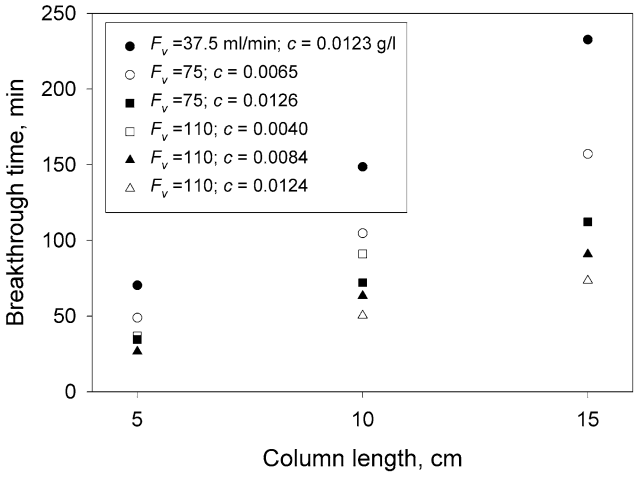

Fig. 4 Breakthrough time as a function of column length and feed flow characteristics at 100 °C

Table 4 Effect of flow rate and influent vapor concentration on coefficients of (5) at $u = 0.1\%$ calculated from dependence of breakthrough time on column length

v/cm min^{-1}	Conc./g l^{-1}	K/min cm^{-1}	t_0/min
59.5	0.0123	16.23	11.81
115	0.0065	10.82	4.66
115	0.0126	7.76	4.67
174	0.0040	10.86	17.47
174	0.0084	6.42	3.87
174	0.0124	4.62	−4.34

tioned (Asnin et al. 2003) that a fraction of high-energy adsorption sites on the surface of Al_2O_3/V_2O_5 is small, an order of magnitude being of $10^{-2}\%$. When the surface coverage is less than this value the decrease of adsorption heat and entropy as functions of adsorbed amount is fast. But beyond this point the functions change insignificantly (Asnin et al. 2001; Asnin and Fedorov 2003). This suggests that the surface becomes quasihomogeneous after covering of the high-energy sites and adsorption equilibrium at such surface can be described by the Langmuir isotherm. A similar phenomenon was observed in several adsorption systems including CB and a polar coadsorbate (water or pyridine) (Murena and Gioia 1998; Demeestere et al. 2003). It played a role of a catalytic poison shielding the sites of strong adsorption that resulted in a quasihomogeneous state of the surface of a solid; the interaction of a target adsorbate with such surface then obeyed to the Langmuir model.

Figure 3 compares breakthrough curves measured with the columns of different lengths at different flow rates at 100 °C. The breakthrough time plotted as a function of the column length (Fig. 4) demonstrates a linear trend according to (5). Correlations between the slope or intercept of these lines and flow characteristics are observed (Table 4) but they make no essential contribution into understanding column dynamics. At the same time, an approach applying the reduced lumped diffusion model described above allows some features of column dynamics to be revealed. Equations (5–8) satisfactory approximate breakthrough curves (Fig. 3), the best-fit values of the model parameters listed in Table 5. Note that the coefficient K derived from this model approximation is in the perfect agreement with the value of definition (Γ/v). Data in the table reveal the following correlations: the external mass transfer coefficient diminishes as the column length increases. It is also a decreasing function of the adsorbate concentration at constant flow velocity and an increasing function of the flow velocity at constant concentration. The latter could be explained taking into account the

Table 5 A summary of mass transfer coefficients at different experimental conditions

v/cm min^{-1}	Conc./g l^{-1}	$\Gamma = q^0/c^0$	K (5)/min cm^{-1}	$K = (\Gamma/v)$/min cm^{-1}	β_e/min^{-1}	$(D/\epsilon_p \overline{D}_{Km})$
$L = 5$ cm						
59.5	0.0123	915	15.3	15.4	1980	0.22
115	0.0065	1323	11.4	11.5	3240	0.66
115	0.0126	908	7.9	7.9	2640	0.44
174	0.0040	1549	9.0	8.9	4680	1.10
174	0.0084	1120	6.4	6.4	3780	0.83
$L = 10$ cm						
59.5	0.0123	963	16.1	16.2	900	0.49
115	0.0065	1357	11.4	11.3	2160	1.55
115	0.0126	953	7.9	8.1	1440	1.42
174	0.0040	1745	9.9	10.0	4440	3.11
174	0.0084	1231	7.0	7.1	2640	1.68
174	0.0124	954	5.6	5.6	1980	1.05
$L = 15$ cm						
59.5	0.0123	1029	17.0	17.3	360	0.47
115	0.0065	1469	12.0	12.1	660	4.01
115	0.0126	1009	8.6	8.7	420	3.24
174	0.0084	1265	7.1	7.3	660	5.96
174	0.0124	1000	5.8	5.8	540	1.11

contraction of the stagnant surface fluid film resulting from the increase of flow velocity. The intraparticle diffusion coefficient is the higher the longer the column. At the same time, it changes as a function of concentration like β_e but shows no plain dependence on the flow velocity. The theoretical effective diffusivity of CB in the pores ($\epsilon_p \overline{D}_{Km}$; see Appendix) is of an order of magnitude of the experimental D value. The apparent tortuosity factor evaluated as the ratio $\epsilon_p \overline{D}_{Km}/D$ ranges from 0.2 to 4.5 depending on experimental conditions. The values of $\tau < 1$ are found in diffusivity studies (Satterfield 1970) and indicate the imperfection of the model. At the same time, the upper limit of the observed tortuosity is reasonable considering that the reported values in the literature range from 2 to 6 (Satterfield 1970), suggesting that model incompleteness has not a dramatic effect on the results.

It is interesting to analyze trends in dimensionless Stanton and Biot numbers (Table 6). The former one ($\mathrm{St} = \beta_e L \epsilon_e / v$) compares the external and convective mass transfer and the latter number ($\mathrm{Bi} = \beta_e d_p/(2a_p D)$) characterizes the relative contribution of the internal and external diffusion in the mass transfer. The Biot number decreases approaching zero as column length extends suggesting a prevailing importance of the external mass transfer resistance over the pore diffusion one for longer beds. It correlates with a progressive rise of the external mass transfer contribution (K_1; see theoretical Sect. 2) to the overall mass transfer resistance ($K_1 + K_2$) from 11–20% for a 5 cm column to 58–90% for a 15 cm column. The Stanton number is a decrescent function of the flow velocity, in spite of $\beta_e(v)$ being an increasing function within the investigated range. This is an expected finding because diffusion kinetics is finite in principle and the flow rate has no theoretical limits to rise.

Kaczmarski et al. (2001) proposed criteria of model adequacy. So, the POR model is considered to be valid if

$$\mathrm{Pe} \succ 100 \qquad \frac{\mathrm{St}}{\mathrm{Bi}} \succ 5 \tag{11}$$

The Peclet number [$\mathrm{Pe} = vL/(D_{ax}\epsilon_e)$] cannot be determined in the framework of the used model because the axial dispersion coefficient D_{ax} is neglected but it can be estimated from Gunn equation (Gunn 1987), the estimates are reported in Table 6. As seen from the table, the conditions of (11) are fulfilled. Hence, no errors originating from assumptions of the POR model may significantly affect the obtained results. It is rather that a further simplification of the model introduces the lumped effect into the determined dynamic coefficients. Among the effects neglected in the reduced model, the axial dispersion, surface diffusion and adsorption-desorption kinetics are the most important to be discussed. Indeed, Eberly and Spencer (1961) studying the elution of benzene vapor through the bed of zeolite found that the influence of the axial dispersion became noticeable when the flow velocity descended below

Table 6 Dimensionless mass transfer numbers

v/cm min^{-1}	Conc./g l^{-1}	St	Bi	St/Bi	Pe
$L = 5$ cm					
59.5	0.0123	73	14.7	5	130
115	0.0065	62	8.0	8	219
115	0.0126	51	9.8	5	
174	0.0040	59	6.9	9	269
174	0.0084	48	7.4	6	
$L = 10$ cm					
59.5	0.0123	67	3.0	22	283
115	0.0065	83	2.3	36	474
115	0.0126	55	1.7	33	
174	0.0040	112	2.3	48	581
174	0.0084	67	2.6	26	
174	0.0124	50	3.1	16	
$L = 15$ cm					
59.5	0.0123	40	1.3	32	442
115	0.0065	38	0.27	141	738
115	0.0126	24	0.21	114	
174	0.0084	25	0.18	138	903
174	0.0124	20	0.79	26	

$\sim$600 cm min^{-1} whereas in our experiments the v value was under 175 cm min^{-1}. We can assess the importance of the axial dispersion using values determined by Gunn equation. A respective resistance term (D_{ax}/v^2) (Dubinin et al. 1969) is less than 5% of the experimental overall mass transfer resistance ($K_1 + K_2$) under any experimental conditions examined. Thus, the neglect of this effect is reasonable. The surface diffusion can be suggested considering a negative relationship between the apparent intraparticle diffusivity and concentration. The separate estimation of the bulk and surface fluxes is difficult and can hardly be done on the basis of the present data. Moreover, the intraparticle mass transfer can be complicated by the influence of the adsorption-desorption kinetics. Although physisorption of polar adsorbates on metal oxide catalysts is believed to be activationless and fast, desorption can be slow if adsorption heat is high, which is the case for a CB-V_2O_5/Al_2O_3 system (Asnin et al. 2001). Frequently, investigators assume an infinite rate of adsorption-desorption to avoid simultaneous consideration of intraparticle diffusion and adsorption phenomena (Golshan-Shirazi and Guiochon 1992). This results in effective intraparticle diffusion coefficients latently including adsorption-desorption rate constants. Such an approach is reasonable because the effect of adsorption is to hinder the migration of an adsorbate inside a catalyst particle and it does not affect the external mass transfer.

The model of discussion is in qualitative agreement with the literature correlations relating the external mass transfer coefficient to the flow velocity (Wakao and Funazkri 1978) and the intraparticle diffusivity to concentration (Dubinin et al. 1969; Satterfield 1970). The dependence of apparent dynamic parameters on column length is also a well known effect in adsorption and chromatographic techniques utilizing packed beds (Koh and Guiochon 1998; Guiochon et al. 1997; Pecsar 1971; Han et al. 1985). Karpovich et al. (1995) in their study of filtering carbon tetrachloride vapors through a bed of a charcoal adsorbent observed a 20% drop in the adsorption rate constant when bed depth increased from 5 to 15 cm. Intensive studies pertaining mainly to a realm of liquid chromatography relates this phenomenon to a nonuniform distribution of the packing density both in the axial and in the radial directions. There are two sources of bed heterogeneity: particle size distribution and the compaction of packed beds. The former is accounted for by the segregation of particles of certain size at certain positions in a column. So, it is found that during dry packing (a method used in the given study) the coarser particles tend to segregate close to the wall of the container (Pecsar 1971; Guiochon et al. 1997). Bed compaction during a packing procedure results in the variation of the packing density in the axial direction unless an appropriate averaging mechanism is applied. Although short columns had been taken for the study we also observed this effect. For column length of 5, 10, and 15 cm the packing density was 0.63, 0.66, and 0.68 g cm^{-3} respectively. The most significant impact of the

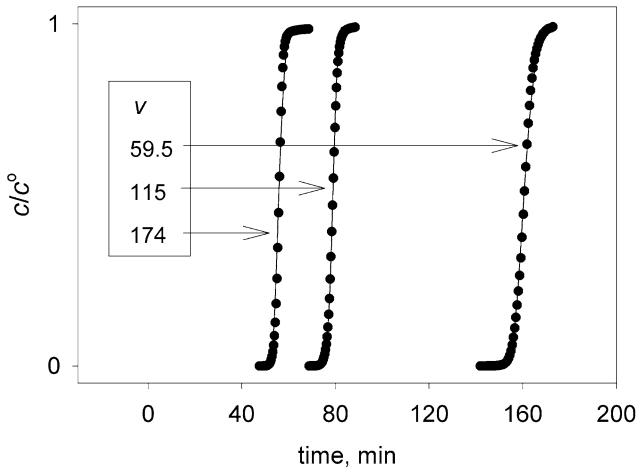

Fig. 5 Comparison of experimental breakthrough curves (*points*) and theoretical profiles calculated using (5–8) and the empirical expressions in Table 7 (*lines*). Column length 10 cm, CB vapor concentration 0.0126 g/l, temperature 100 °C

Table 7 Empirical models of mass transfer coefficients

$D = \delta_0 + \delta_1 L + \delta_2 v + \delta_{12} Lv + \delta_{13} Lc + \delta_{122} Lv^2 + \delta_{123} Lvc$

$\beta_e = \beta_0 + \beta_1 L + \beta_2 v + \beta_3 c$

$\delta_0 = 0.36$	$\beta_0 = 4970$
$\delta_1 = -0.6$	$\beta_1 = -252$
$\delta_2 = -0.0066$	$\beta_3 = 9$
$\delta_{12} = 0.0084$	$\beta_3 = -1.66 \cdot 10^5$
$\delta_{13} = 34.2$	$R^2 = 0.91$
$\delta_{122} = -1.6 \cdot 10^{-5}$	
$\delta_{123} = -0.31$	
$R^2 = 0.87$	

bed nonuniformity on column dynamics especially for short columns is likely to be connected to the inequality of conditions for such mechanisms of axial dispersion as the "wall effect" and eddy diffusion in columns of different lengths. It seems that this circumstance explains in part the results of the given study. Consideration of this phenomenon in terms of dynamic models requires knowledge of the axial and radial particle size and external porosity distributions, which information is rarely obtainable.

Since dynamic coefficients depend on experimental conditions and column length the use of the considered model to predict breakthrough curve under arbitrary conditions is difficult. To overcome this obstacle an analytical relationship between the dynamic coefficients and influencing factors should be found. Multiple regression analysis delivers such expressions as shown in Table 7. Whereas a function $\beta_e(L, c, v)$ is satisfactory linear, a polynomial equation with interaction terms approximates a dependence of D on the same factors. Figure 5 demonstrates perfect agreement between experimental breakthrough curves and those calculated using the model under discussion supplemented with the expressions found for β_e and D.

5 Conclusions

Equilibrium adsorption capacity of a 5% V_2O_5/Al_2O_3 catalyst with respect to CB vapor obeys to the Langmuir equation within the concentration range investigated. This is not supposed to be a result of the surface homogeneity but is caused either by a narrow interval of adsorbate concentration explored or by shielding of the high-energy adsorption sites that results in a quasihomogeneous state of the surface. The exceeding of equilibrium adsorption capacity over the breakthrough one is not influenced by experimental conditions and is of $\sim 13\%$ for the given size of the catalyst's particles.

Column dynamics is described by the reduced lumped diffusion model that should be regarded here as an empirical one because the dynamic parameters of the model are functions of experimental conditions and the column length in contradiction with assumptions of the model. Nevertheless, it has its advantage of prognostic ability and can be used to predict breakthrough curves once expressions relating β_e and D to the flow velocity, adsorbate concentration and column length are found.

Acknowledgements This work was supported by grants of RFBR (No. 06-03-32525) and of Russian Science Support Foundation. Authors thank prof. K. Kaczmarski (Rzeszów University of Technology, Rzeszów, Poland) for fruitful discussions.

Appendix

The combined diffusivity, $D_{Km}(r)$ inside the pores of radius r is given by a combination of both Knudsen ($D_K(r)$) and molecular (D_m) diffusivities as:

$$\frac{1}{D_{Km}(r)} = \frac{1}{D_K(r)} + \frac{1}{D_m}$$

where molecular diffusivity is equal to 7.2 $cm^2\ min^{-1}$ as estimated by Fuller-Schettler-Giddings expression (Fuller et al. 1966) and Knudsen diffusivity is $D_K(r) = 9700r \cdot [(T + 273)/M]^{0.5}$. The value averaged over the pore size distribution is found as:

$$\overline{D}_{Km} = \int_{r_1}^{r_2} D_{Km}(r) f(r) dr$$

where $f(r)$ is the distribution function, r_1 and r_2 are the lower and upper limits of the experimental pore size distribution.

References

Akulov, A.K., Grebenschikov, S.F., Pakhomov, Yu.I.: Modeling the dynamics of adsorption on activated carbon-fibers. J. Appl. Chem. USSR **59**, 1142–1146 (1986)

Asnin, L.D., Fedorov, A.A.: Adsorption of chlorobenzene on γ-Al_2O_3 obtained by calcination of boehmite at various temperatures. Russ. J. Appl. Chem. **76**, 719–722 (2003)

Asnin, L.D., Fedorov, A.A., Checryshkin, Yu.S., Yakushev, R.M.: Adsorption of chlorobenzene on catalyst V_2O_5/γ-Al_2O_3. Russ. J. Appl. Chem. **74**, 1458–1460 (2001)

Asnin, L.D., Fedorov, A.A., Checryshkin, Yu.S.: Adsorption of benzene on the V_2O_5/γ-Al_2O_3 catalyst. Russ. Chem. Bull. **52**, 889–892 (2003)

Chintavar, P.S., Green, H.L.: Adsorption and catalytic destruction of trichloroethylene in hydrophobic zeolites. Appl. Catal. B **14**, 37–47 (1997)

Davidenko, I.V., Davydov, A.A., Pyatnitskii, Yu.I., Belokopytov, Yu.V., Agazade, A.G.: Study of chlorobenzene transformations on the surface of oxide vanadium catalyst by the methods of IR-spectroscopy and thermodesorption. Teor. Eksp. Khim. **26**, 468–473 (1990)

Davidenko, I.V., Davydov, A.A., Pyatnitskii, Yu.I., Belokopytov, Yu.V., Agazade, A.G.: Forms of benzene and its chlorine-derivatives adsorption on the oxide vanadium catalyst surface. Zh. Fiz. Khim. **65**, 164–169 (1991)

Demeestere, K., Dewulf, J., van Langenhove, H., Sercu, B.: Gas-solid adsorption of selected volatile organic compounds on titanium dioxide Degussa P25. Chem. Eng. Sci. **58**, 2255–2267 (2003)

Dubinin, M.M., Lezin, Yu.S., Zikanova, A.: Dynamics of isothermal adsorption in a system of parallel transport with a variable coefficient of internal mass exchange. Russ. Chem. Bull. **18**, 441–445 (1969)

Eberly, P.E., Spencer, E.H.: Mathematics of adsorption for pulse flow through packed columns. Trans. Faraday Soc. **57**, 289–300 (1961)

Everaert, K., Baeyens, J.: Catalytic combustion of volatile organic compounds. J. Hazard. Mater. **B109**, 113–139 (2004)

Fedorov, A.A., Chekryshkin, Yu.S., Shadrina, N.G.: Adsorption and catalytic oxidation of chlorobenzene on highly permeable cellular systems. Russ. J. Appl. Chem. **71**, 1942–1945 (1998)

Fuller, E.N., Schettler, P.D., Giddings, J.C.: New method for prediction of binary gas-phase diffusion coefficients. Ind. Eng. Chem. **58**, 18–27 (1966)

Han, N.-W., Bhakta, J., Carbonell, R.G.: Longitudinal and lateral dispersion in packed beds: Effect of column length and particle size distribution. AIChE J. **31**, 277–288 (1985)

Golshan-Shirazi, S., Guiochon, G.: Comparison of the various kinetic models of non-linear chromatography. J. Chromatogr. A **603**, 1–11 (1992)

Guiochon, G.: Preparative liquid chromatography. J. Chromatogr. A **965**, 129–161 (2002)

Guiochon, G., Farkas, T., Guan-Sajonz, H., Koh, J.-H., Sarker, M., Stanley, B.J., Yun, T.: Consolidation of particle beds and packing of chromatographic columns. J. Chromatogr. A **762**, 83–88 (1997)

Gunn, D.J.: Axial and radial dispersion in fixed bed. Chem. Eng. Sci. **42**, 363–373 (1987)

Jones, J., Ross, J.R.H.: The development of supported vanadia catalysts for the combined catalytic removal of the oxides of nitrogen and of chlorinated hydrocarbons from flue gases. Catal. Today **35**, 97–105 (1997)

Kaczmarski, K., Antos, D., Sajonz, H., Sajonz, P., Guiochon, G.: Comparative modeling of breakthrough curves of bovine serum albumin in anion-exchange chromatography. J. Chromatogr. A **925**, 1–17 (2001)

Karpovich, F., Hearn, J., Wilkinson, M.C.: The quantitative use of the Bohart-Adams equation to describe effluent vapour profiles from filter beds. Carbon **33**, 1573–1583 (1995)

Koh, J.-H., Guiochon, G.: Effect of the column length on the characteristics of the packed bed and the column efficiency in a dynamic axial compression column. J. Chromatogr. A **796**, 41–57 (1998)

Krishnamoorthy, S., Amiridis, M.D.: Kinetic and in situ FTIR studies of the catalytic oxidation of 1,2-dichlorobenzene over V_2O_5/Al_2O_3 catalysts. Catal. Today **51**, 203–214 (1999)

Krishnamoorthy, S., Baker, J.P., Amiridis, M.D.: Catalytic oxidation of 1,2-dichlorobenzene over V_2O_5/TiO_2-based catalysts. Catal. Today **40**, 39–46 (1998)

Lukin, V.D., Novoselskii, A.V.: Ciklicheskie adsorbcionnye processy [Cyclic adsorption processes], pp. 58–80. Khimiya, Leningrad (1989)

Morbidelli, M., Storti, G., Carra, S., Niederjaufner, G., Pontoglio, A.: Study of a separation process through adsorption of molecular sieves. Chem. Eng. Sci. **39**, 383–393 (1984)

Murena, F., Gioia, F.: Catalytic hydroprocessing of chlorobenzene-pyridine mixtures. J. Hazard. Mater. **60** 271–285 (1998)

Pecsar, R.E.: Preparative column technology. In: Zlatkis, A., Pretorius, V. (eds.) Preparative Gas Chromatography. Wiley-Interscience, New York (1971), Chap. 3

Satterfield, C.N.: Mass Transfer in Heterogeneous Catalysis. MIT Press, Cambridge (1970), Chap. 1

Shim, W.G., Choi, D.Y., Choi, S.P., Lee, J.-W., Moon, H.: Column dynamics of benzene vapor adsorption on MCM-48. Adsorption **11**, 503–507 (2005)

Xia, Q.-H., Hidajat, K., Kawi, S.: Adsorption and catalytic combustion of aromatics on platinum-supported MCM-41 materials. Catal. Today **68**, 255–262 (2001)

Wakao, N., Funazkri, T.: Effect of fluid dispersion coefficients on particle-to-fluid mass transfer coefficients in packed beds. Correlation of Sherwood numbers. Chem. Eng. Sci. **33**, 1375–1384 (1978)

Zagoruiko, A.N., Kostenko, O.V., Noskov, A.S.: Development of the adsorption-catalytic reverse-process for incineration of volatile organic compounds in diluted waste gases. Chem. Eng. Sci. **51**, 2989–2994 (1986)